PRFS-based MR thermometry is hampered by susceptibility changes caused by the heating of fat: Experimental demonstration

S. M. Sprinkhuizen[1], C. J. Bakker[1], and L. W. Bartels[1]
[1]Radiology, Image Sciences Institute, Utrecht, Utrecht, Netherlands

Introduction In the application of proton resonance frequency shift (PRFS)-based MRT during thermal interventions, the contribution of susceptibility related field changes on the water PRF is commonly ignored. The magnetic volume susceptibility χ of tissue is, however, temperature dependent. For water, the temperature dependence of χ is in the order of 0.002 ppm/ºC [1]. For fat, this is even more substantial, and in the same order of magnitude as the temperature dependence of the chemical shift of water which is exploited for PRFS-based MRT (0.0094 ppm/ºC [2]). PRFS-based MR temperature measurements may therefore be corrupted by nonlocal magnetic field effects due to temperature-induced susceptibility changes in fat tissue. This raises a realistic problem during thermal interventions in tissues where fat is present, e.g. breast tissue. To investigate the influence of the temperature dependence of the susceptibility of fat on PRFS-based MRT maps, a heating experiment was conducted in a phantom set-up.

Materials & Methods All scans were performed on a 1.5-T whole body MRI scanner (Achieva, Philips Healthcare, Best, The Netherlands). The phantom consisted of a large circular container, filled with water (doped with $MnCl_2$), in which a Perspex cylinder (outer radius = 20 mm; inner radius = 16 mm; length = 84 mm) was placed, such that the long axis of the cylinder was aligned perpendicular to the direction of the main magnetic field. The cylinder was filled with sunflower oil. At the start of the experiment, the temperature of the water in the outer container was equal to the temperature of the oil within the cylinder (~18 ºC). A total of 70 PRFS-based MRT scans were acquired of a coronal 2D single slice through the center of the cylinder (FOV 320x320 mm^2; acq. voxel size: 2x2x4 mm^3; flip angle $\alpha = 30^o$; water fat shift = 0.5 pixels; TE = 15 msec; TR = 50 msec; scan duration = 8 sec). During the first five PRFS-based MRT scans, the phantom was kept at constant temperature. After the acquisition of the fifth scan and prior to the sixth scan, the oil in the cylinder was quickly replaced with the same, but pre-heated, oil ($\Delta T \approx 30$ ºC).
The phantom set-up was designed such that the susceptibility-related temperature errors in the PRFS-based temperature maps were expected to appear in a dipole-pattern around the cylinder. This is shown by the following equation which gives the microscopic field change (ΔB) outside of a cylinder (perpendicular to B_0) caused by susceptibility changes:

$$\Delta B = \frac{\Delta\chi_e}{3} + \frac{\Delta\chi_e - \Delta\chi_i}{2} R^2 \frac{(x^2 - z^2)}{(x^2 + z^2)^2}$$

with R the radius of the cylinder and $\Delta\chi_e$ and $\Delta\chi_i$ the susceptibility changes outside and inside of the cylinder, respectively. This equation shows that, for a coronal PRFS-based temperature map and $\Delta\chi_e = 0$, a positive $\Delta\chi_i$ leads to positive field offsets in the direction of z (B_0), and to negative field offsets over the x-axis. This corresponds to a temperature underestimation over the z-axis and a temperature overestimation over the x-axis, due to the negative relation between PRF and temperature (3). To validate the true temperature during all scans at these two specific locations around the cylinder (location 1 and 2, respectively), two optical temperature fibers were positioned at ~1.5 mm from the edge of the cylinder (figure 1b).
A third optical fiber was positioned in the outer container, and used for field drift correction, together with the phase information at that same location. After drift correction, the PRFS-based temperature was averaged within a region of interest (2 voxels) at locations 1 and 2 for all scans. The temporal and spatial behavior of the PRFS-based temperature in the water surrounding the cylinder was then compared to the temperature measured with the optical fibers.

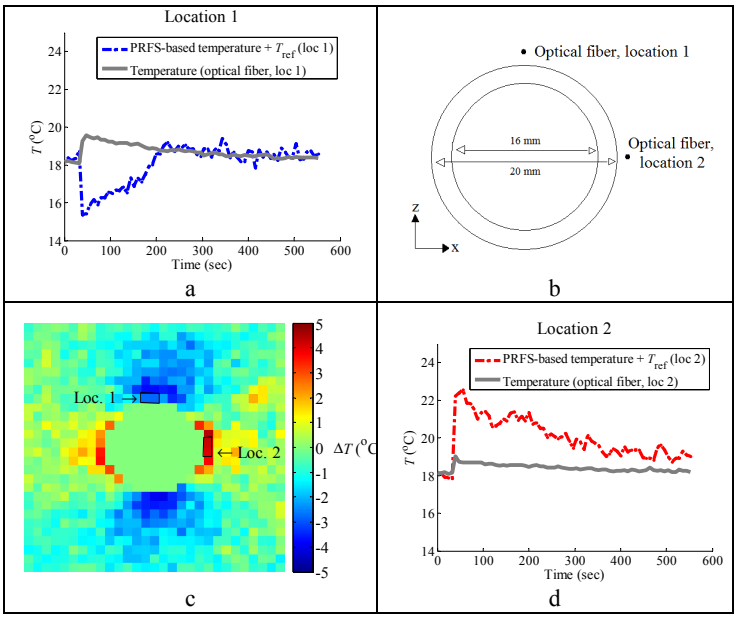

Figure 1. The PRFS-based temperature map of the first scan after administration of heated oil inside the cylinder, is shown (partially) (c). The two regions from which the average temperature signal over time was taken are indicated by black boxes. At these two locations, optical fiber temperature measurements were acquired (b). Per location, the optical temperature is compared to the (drift-corrected) PRFS-based temperature (a and d) over time.

Results In figure 1c, the PRFS-based temperature map of scan number 6 (fig. 1c) is shown. For visual purposes, water-voxels are depicted only, by setting all voxels containing fat (inside the cylinder) to zero. This temperature map clearly shows a dipole field pattern around the cylinder, which indicates that the temperature measurements in water are hampered by the nearby heated fat. The PRFS-based temperature profiles over time are compared with the true optically measured temperature at two locations (fig. 1a and 1d). Note that the starting temperature (as measured with the optical fibers) is added to the PRFS temperature profiles (which contain temperature changes only). The dipole-behavior is clearly apparent based on these figures: at location 1, the true temperature increases with 1.5 ºC, whereas the measured PRFS-based temperature decreases with 3.5 ºC. At location 2, the true temperature increases with 1 ºC, whereas the PRFS-based temperature increases with 5 ºC.

Discussion and conclusion The experimental results provided proof for the fact that susceptibility changes in fat hamper the PRFS-based MRT method nonlocally. The measured errors were ranging between -4.6 ºC and +4.1 ºC. We would like to stress the fact that fat suppression is not a solution for this effect.

References [1] Philo JS *et al.* J. Chem. Phys. 1980;72:4429 [2] de Poorter J. Magn Reson Med. Sep 1995;34(3):359-67 [3] Hindman JC. J. Chem. Phys. 1966;44:4582-4592 [4] Hopkins J. Magn Reson Med. 1997 Apr;37(4):494-500 [5] Sprinkhuizen SM *et al.* Proc. #2532 ISMRM 17 (2009) [6] Moerland MA *et al.* Phys. Med. Biol. 1995;40:1651-1664